Bull. Mater. Sci. (2019) 42:261
https://doi.org/10.1007/s12034-019-1940-z

Band structure and thermoelectric properties of Cu_2O from GGA and GGA+U approaches

V MAURYA* and K B JOSHI
Department of Physics, M. L. Sukhadia University, Udaipur 313001, India
*Author for correspondence (vijaymaurya2414@gmail.com)

MS received 15 October 2018; accepted 29 January 2019

Abstract. Electronic band structures and thermoelectric (TE) properties of cuprous oxide crystallizing in the *Pn*3*m* space group are investigated using the linearized augmented plane wave method. The generalized gradient approximation (GGA) and GGA+U approaches are adopted for calculations at the level of the density functional theory. After achieving the ground state of the crystal, the electronic band structures are calculated. The *ab initio* calculations are interfaced with the Boltzmann transport equations to unveil TE properties. We have found the Seebeck coefficient, power factor and electrical conductivity to compute the electronic fitness function (EFF) further. The effect of temperature is also studied. The EFF suggests that the material may become a useful TE material after p-type doping.

Keywords. Cuprous oxide; electronic band structure; thermoelectric properties.

1. Introduction

Among several crystals of cuprous oxide (Cu_2O), the cuprite phase is the most important due to technological applications [1–4]. Although most of the crystals are semiconductors, cuprite is used in photovoltaic conversion and cost-effective solar cells [5,6]. Along with several other metal oxides, the surface properties are studied to see corrosion of metals, usage in catalytic processes and gas sensors [7]. Oxides of copper are preferred owing to their non-toxic nature. The p-type Cu_2O is useful in thin film transistors and in optoelectronic, nanoelectronic, spintronic and photovoltaic applications [5,7]. Under ambient conditions, Cu_2O crystallizes in the cuprite structure [1,2,8]. This phase of Cu_2O is also being explored to see the thermodynamic and thermoelectric (TE) properties [4,8–10]. Attempts are also made to tailor the TE properties by means of doping. Thus, to bring the performance of Cu_2O to a useful level, more work is required.

In transition metal oxides, it is observed that *ab initio* quantum mechanical methods based on the density functional theory (DFT) do not adequately describe the electronic properties using local density approximation. DFT calculations under generalized gradient approximation (GGA) give improved results yet show some deviation from experimental data. There is a divergence in the calculated band gaps and discrepancies in the ordering of conduction bands. Therefore, the GGA+U calculations are also in practice [2,11,12]. These are considered adequate to correctly describe relatively localized d-states in transition metal compounds. In this approach, an on-site Coulomb repulsion, the Hubbard U term, is added to include the self-interaction correction with localized d-states following a standard theoretical formalism [11–14]. In this work, we consider both GGA and the GGA+U calculations.

We deploy the full-potential linearized augmented plane wave (FP-LAPW) method founded on the DFT [15]. The Kohn–Sham (KS) E–k eigen-spectra from the FP-LAPW method are interfaced with the BoltzTraP scheme and the transport coefficients are found [16,17]. Only recently, it was proposed that the suitability of a semiconductor as a TE material can be judged by the electronic fitness function (EFF) [18]. The function provides the degree to which the band structure can be decoupled with electrical conductivity (σ) and Seebeck coefficient (S), which otherwise have counterpoising roles in ascertaining the TE properties, especially the figure of merit and the power factor (PF $= \sigma S^2$). The function is known to capture the behaviour that quantifies the favourable TE performance. It is very useful to see the utility of a semiconductor as the TE material. In this extended work, we give the electronic band structures and use the transport coefficients to evaluate EFF and its variation with carrier concentration [19]. EFF is compared with other similar compounds and a few most promising TE materials.

2. Computational method

2.1 *Crystal structure and methodology*

The cuprite structure of Cu_2O belongs to the space group *Pn*3*m*. It contains two formula units per primitive cell. Calculations are performed by applying the FP-LAPW method. The Perdew–Burke–Ernzerhof (PBE) ansatz based on the GGA is

Published online: 11 September 2019

considered to treat the exchange and correlation part of the KS Hamiltonian [20]. The muffin-tin radii were 1.97 and 1.478 Bohr for Cu and O atoms, respectively. The plane wave cut-off parameter *rgkmax* was set to 8.5. Both the GGA and GGA+U calculations are performed at the lattice constant $a = 4.28$ Å as described in our earlier work [19]. In the GGA+U calculations, the Hubbard U_{eff} parameter is $U_{\text{eff}} = U - J$, where U and J are the screened Coulomb and exchange parameters [14]. Several combinations of U and J were tried and the optimum values of the lattice constant, bulk modulus and band gap were found for $U_{\text{eff}} = 8$ eV [19]. The U parameters considered by other workers [21] in the GGA (PBE)+U calculations alter the lattice constant merely by 1.2%. So, current GGA+U calculations are performed at the same lattice constant.

2.2 *Transport properties*

The conversion efficiency from heat to electricity of a TE material is defined by a figure of merit, $ZT = \sigma S^2 T/\kappa$, where S is the Seebeck coefficient or thermopower, and κ is the thermal conductivity ($\kappa_e + \kappa_l$), which is the sum of electronic thermal conductivity (κ_e) and lattice thermal conductivity (κ_l). A number of possibilities can be realized to obtain high ZT. For instance, there may be a combination of high σ, high S or high σ and low κ.

To compute the TE properties, the Boltzmann semi-classical transport equations are interfaced with the KS E–k spectrum generated by the *ab initio* calculations. The procedure requires energy eigen-values at a mesh of highly dense k-points. Therefore, in both GGA and GGA+U calculations, a grid of $76 \times 76 \times 76$ is used in the LAPW method [15]. The eigen-energies at 10,660 k-points in the irreducible Brillouin zone were calculated. These band energies were enough to ensure convergence in Fourier expansion coefficients. The calculations are performed following the two approximations. Firstly, the constant relaxation time approximation (CRTA) $\tau_{i,k} = \tau$, and secondly, the rigid-band approximation (RBM). In both approximations, it is assumed that the band dispersions do not vary with temperature or doping.

The TE quantities are obtained from the average of the diagonal components of the Seebeck coefficient and electrical conductivity tensors. S and electrical conductivity, σ, are then used to predict the power factor (PF $= S^2\sigma$). The EFF proposed very recently is defined as $t = (\sigma/\tau)S^2\ (N/V)^{2/3}$ [18]. Here, τ is the relaxation time, and σ/τ and S are obtained directly from the band structure and Boltzmann transport equations. σ and τ separately require detailed knowledge of the scattering. EFF provides a clue on the basis of band structure data to decouple σ and S to tailor PF and the figure of merit. EFF can be directly evaluated from the transport coefficients deduced from the Boltzmann transport theory [22,23]. The function has been very useful in filtering promising TE materials from a large number of oxides and half metallic alloys [18,22,23]. In the EFF, (N/V) is the volumetric density of states that is proportional to the density of states effective mass, and Fermi energy as $(N/V) \sim (m^*_{\text{dos}})^{3/2} E_F^{1/2}$ for a parabolic band. E_F is relative to the band edge and m^*_{dos} is the effective mass of the density of states [24]. In this work, we calculate this useful function by generating the band structure from the GGA and GGA+U approaches. It will enable one to see the utility of Cu_2O as a TE material and marks position on the EFF scale in the list of other useful TE materials. It is insightful to analyse the counterpoising roles of σ and S through complex shapes and other features of the band structure in TE behaviour. The unit of this complex EFF is $W^{5/3}\ ms^{-1/3}\ K^{-2}$ in the SI system.

3. Results and discussion

3.1 *Electronic band structure*

The electronic band structures from GGA and GGA+U are presented orderly in figures 1 and 2. In both the structures, the Cu-3d, 4s and O-2p electrons play a critical role in the formation of bands visible in drawings. The Cu-3d band largely constitutes the region between 0 and −4.5 eV. In the region −5 to −7.5 eV, not shown in the figure, the major contribution is from the O-2p state. The band gap is 0.51 eV from the GGA calculation. The GGA+U does not alter the nature of the band gap, and topologically the band structure is nearly the same. The band gap, however, rises to 0.81 eV, which is still lower than the experimental gaps. Thus, interaction *via* the U term does not open the band gap adequately. It, however, enhances the width of the valence bands between −1 and −2 eV as shown in figure 2.

One can also see the changes in dispersion of the upper valence bands (0 to −2 eV) around the symmetry point R. The top valence band has mixed Cu-3d, 4s and O-2p character and the conduction band has mixed Cu-3d, Cu-4s and O-3s character. The GGA+U potential affects the Cu-3d electrons and the remaining electrons are treated under the GGA. We see band splitting in the 3d-dominated region. Similar

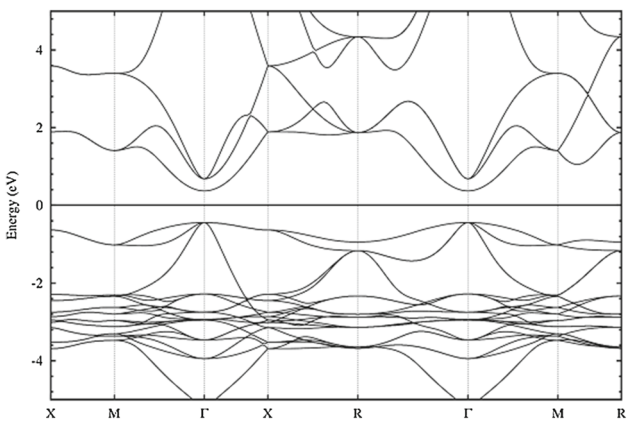

Figure 1. The band structure of cuprite from GGA. The Fermi level lies in the middle of the band gap.

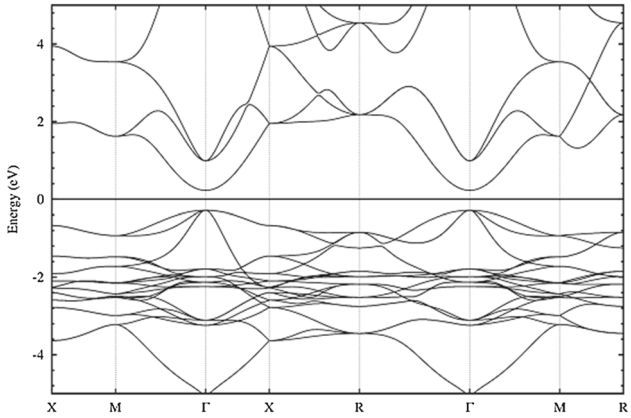

Figure 2. The band structure of cuprite from GGA+U. The Fermi level lies in the middle of the band gap.

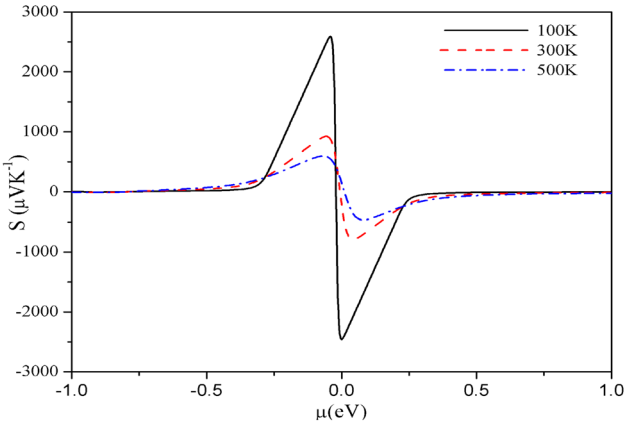

Figure 3. Variation of the Seebeck coefficient with chemical potential at three temperatures. The results are deduced from GGA.

Table 1. The calculated band gaps together with other calculated and measured values. *Source:* Isseroff and Carter [21], Ghijsen *et al* [25] and Shen *et al* [26].

	Band gap (eV)
This work	
GGA	0.51
GGA+U	0.81
Theory	
GGA	0.43 [21]
QP-peak (GGA)	1.39 [21]
GGA+U	0.84 [21]
QP-peak (GGA+U)	1.85 [21]
Experiment	
XPS measurement	2.04 [25]
XPS measurement	2.17 [26]

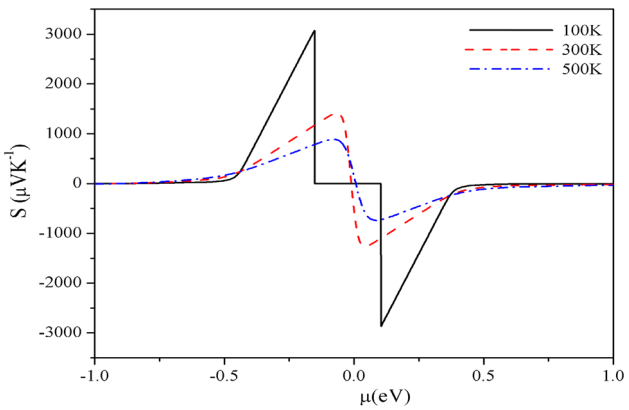

Figure 4. Variation of the Seebeck coefficient with chemical potential at three temperatures. The results are deduced from GGA+U.

observations are reported in earlier studies [21]. A further opening in the band gap can be anticipated by an interaction treating the t_{2g} and e_g electrons differently. Although it is not fully understood, hybrid functionals such as PBE0 may perhaps play such a role [12].

In table 1, calculated and other reported values of the band gap are listed. The calculated band gap is lower than the experimental gaps [25,26]. Other calculations also show such a difference. Notably, the gap is well within the range of 0.43–0.7 eV suggested by a number of GGA calculations [7,8,11,12,21]. With regard to the GGA+U calculations, the current value is very close to the similar calculations performed using the Vienna Ab initio simulation package [21]. Both calculations, however, show deviations from the experiments. The quasi-particle (QP) calculations reduce the gap between theory and experiment, yet a difference of 14.7% remains.

3.2 *Transport coefficients*

In figure 3, the dependence of the Seebeck coefficient, calculated from the GGA approach, on the chemical potential is shown. These are evaluated at 100, 300 and 500 K. Corresponding data from the GGA+U approach are shown in figure 4.

The magnitude of S is almost the same in both the curves. The optimum value of S from GGA lies in the range of $154-344\,\mu V\,K^{-1}$ for 100–500 K. The GGA+U gives the optimum S within $300-512\,\mu V\,K^{-1}$. The recently reported value of $200\,\mu V\,K^{-1}$ by Chen *et al* [10] is well in line with our results. For a complete description of transport coefficients, we need a reasonable value of the relaxation time (τ). This is found from the available experimental data described in our earlier work [19]. We found $\tau = 6.13 \times 10^{-15}$ s and 2.47×10^{-17} s at 300 and 500 K, respectively. It may be mentioned that the accurate relaxation time may be obtained if conductivity measurements are performed by varying the concentration as well as temperature and no such data are

available for cuprite. The computed PF and its concentration dependences clearly show that holes are the majority charge carriers in cuprite and carrier compensation is less effective, which makes cuprite a suitable TE material in principle [24]. PF also directly appears in EFF. The calculated PF is of the order of 10^{-5} and the values from GGA are within $(0.09-11.3) \times 10^{-5}$ W m^{-1} K^{-2} and from GGA+U, it lies in the range of $(0.12-15.3) \times 10^{-5}$ W m^{-1} K^{-2}.

3.3 *EFF*

Within the validity of CRTA and RBM, one can calculate the TE properties. As mentioned earlier, to determine correct values of σ and PF, the appropriate value of τ is required. In our earlier calculations, the scattering by phonons is not included, which may be effective at high T and high doping levels. EFF describes the electronic aspect of TE performance. It is helpful in filtering the materials that overcome the inverse relationship between electronic conductivity and thermo-power to give better TE performance. It is examined from the salient features embodied in the complex band structure. Although such an effort has been tried by some workers in oxides following a different approach [22,23], EFF has been quite successful for such filtering amongst a large number of materials [18,23]. One can use this function at various doping levels as well as temperatures. EFF is emerging as a universal function which incorporates significant features of the band structure.

In figure 5, the value of EFF calculated by means of GGA and GGA+U is plotted. In the region of low carrier concentration, EFF is almost constant. After 10^{20} cm^{-3} concentration, the function starts to decrease and becomes negligible at 10^{22} cm^{-3}. We have also included the scissor correction in the TE coefficients computed from the band structures using GGA and GGA+U approaches. The scissor correction corrects for the difference in the calculated and measured values of the band gap [9,16,19]. We have calculated the EFF incorporating the scissor correction in the two sets of calculations. The data are presented in table 2. The EFF of FeNbSb is also included because p-type materials having EFF more than FeNbSb are considered as the potential promising TE materials [18].

The t values of other similar transition metal oxide ZnO and the well-known TE compound Bi_2Te_3 are also listed. We note that in cuprite the EFF rises only in GGA when the scissor correction is applied. The effect of this correction is negligible on the EFF obtained from the GGA+U approach. None of the calculations suggests that Cu_2O qualifies as a suitable TE material. However, cuprite is a better TE material than ZnO. It is obvious from table 2 that all t-values of cuprite are below the lower bound. It is worth noting that the EFF bounds of FeNbSb away from the band edge are 0.41 and 1.36 at 300 and 800 K, respectively. These values can be achieved at higher p-type carrier concentration. Thus, the TE performance of cuprite can be enhanced by p-type doping. It is desired that temperature dependent measurements of transport coefficients at various doping levels are available for a number of well-known TE compounds. It will enable to examine the EFF scale from an experimental point of view. It is hoped that this work will invite further work in this direction.

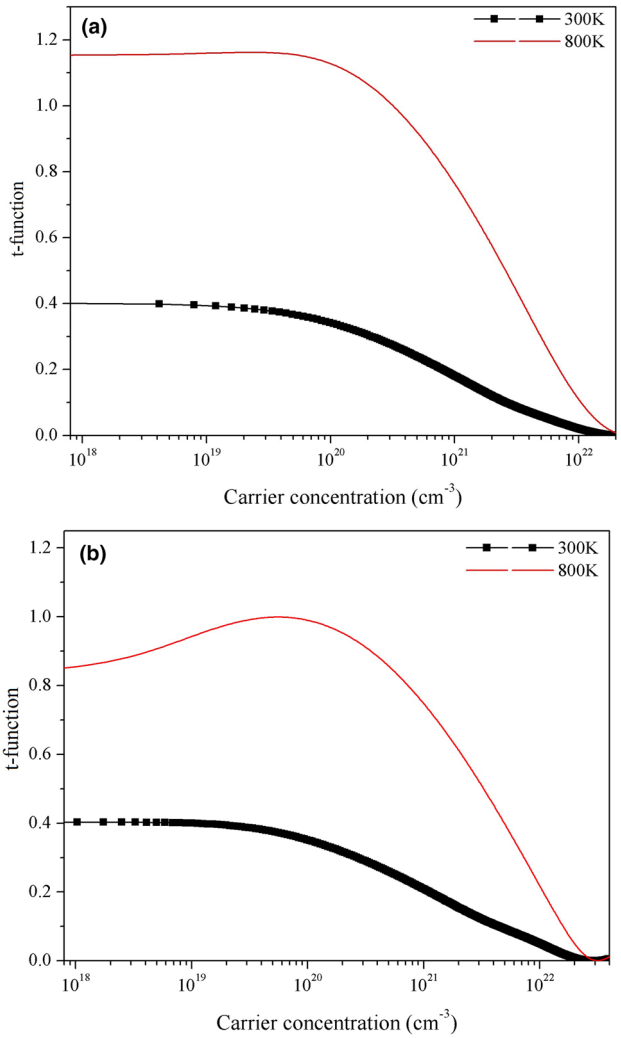

Figure 5. The value of EFF, t with respect to the p-type carrier concentration of Cu_2O at 300 and 800 K, deduced from (**a**) GGA and (**b**) GGA+U approaches.

Table 2. Values of EFF; the t-function (10^{12} W$^{5/3}$ ms$^{-1/3}$ K^{-2}) for some compounds. *Source*: The other data are taken from ref. [18].

	300 K	500 K	800 K
Cu_2O			
GGA	0.40	0.76	1.16
GGA (scissor correction)	0.48	0.83	1.28
GGA+U	0.40	0.67	1.00
GGA+U (scissor correction)	0.40	0.67	1.00
FeNbSb	0.75	—	2.10
ZnO	0.29	—	1.00
Bi_2Te_3	1.80	—	2.89

4. Conclusion

The transport coefficients of cubic Cu_2O are calculated by interfacing the band structure with the Boltzmann transport equations. The GGA and GGA+U approaches are applied to obtain the band structures. The direct electronic band gap is 0.51 and 0.81 eV from the GGA and GGA+U approaches, respectively. The optimum value of the Seebeck coefficient from GGA lies within $154-344\,\mu V\,K^{-1}$. The GGA+U gives the optimum Seebeck coefficient in the range of $300-512\,\mu V\,K^{-1}$. It is in agreement with the findings of Chen *et al* [10] who reported $200\,\mu V\,K^{-1}$ at 300 K. The optimum PF from GGA is within $(0.09-11.3)\times 10^{-5}\,W\,m^{-1}\,K^{-2}$. The GGA+U gives it in the range of $(0.12-15.3)\times 10^{-5}\,W\,m^{-1}\,K^{-2}$. The utility of Cu_2O on the basis of EFF does not qualify Cu_2O as a suitable TE material. It may, however, be noted that it is above ZnO on the EFF scale. We found that the TE performance can be enhanced by p-type doping and may probably be brought to the level of a modest TE material. Temperature dependent measurements of transport coefficients at various doping levels shall be fruitful for further rigorous study.

Acknowledgements

VM is thankful to the UGC, New Delhi for granting the SRF under its BSR scheme. This work is also partially supported by the UGC-SAP and RUSA grants.

References

[1] Meyer B K *et al* 2012 *Phys. Status Solidi B* **249** 1487
[2] Heinemann M, Eifert B and Heiliger C 2013 *Phys. Rev. B* **87** 115111
[3] Hartung D, Gather F, Hering P, Kandzia C, Reppin D, Polity A *et al* 2015 *Appl. Phys. Lett.* **106** 253901
[4] Wong T S K, Zhuk S, Masudy-Panah S and Dalapati G K 2016 *Materials* **9** 271
[5] Rai B P 1988 *Sol. Cells* **25** 265
[6] Chen L C 2013 *Mater. Sci. Semicond. Process.* **16** 1172
[7] Nandy S, Banerjee A N, Fortunato E and Martins R 2013 *Rev. Adv. Sci. Eng.* **2** 273
[8] Zemzemi M, Elghoul N, Khirouni K and Alaya S 2014 *JETP* **118** 235
[9] Young A P and Schwartz C M 1969 *J. Phys. Chem. Solids* **30** 249
[10] Chen X, Parker D, Du M H and Singh D J 2013 *New J. Phys.* **15** 043029
[11] Raebiger H, Lany S and Zunger A 2007 *Phys. Rev. B* **76** 045209
[12] Linnera J and Karttunen A J 2017 *Phys. Rev. B* **96** 014304
[13] Liechtenstein A I, Anisimov V I and Zaanen J 1995 *Phys. Rev. B* **52** R5467
[14] Dudarev S L, Botton G A, Savrasov S Y, Humphreys C J and Sutton A P 1998 *Phys. Rev. B* **57** 1505
[15] http://elk.sourceforge.net/
[16] Madsen G K H and Singh D J 2006 *Comput. Phys. Commun.* **175** 67
[17] Seeger K 2004 *Semiconductor physics* 9th edn (Berlin: Springer)
[18] Xing G, Sun J, Li Y, Fan X, Zheng W and Singh D J 2017 *Phys. Rev. Mater.* **1** 065405
[19] Maurya V and Joshi K B 2019 *J. Alloys Compd.* **779** 971
[20] Perdew J P, Burke K and Ernzerhof M 1996 *Phys. Rev. Lett.* **77** 3865
[21] Isseroff L Y and Carter E A 2012 *Phys. Rev. B* **85** 235142
[22] Xing G, Sun J, Ong K P, Fan X, Zheng W and Singh D J 2016 *APL Mater.* **4** 053201
[23] Sun J and Singh D J 2017 *J. Mater. Chem. A* **5** 8499
[24] Pei Y, Wang H and Snyder G J 2012 *Adv. Mater.* **24** 6125
[25] Ghijsen J, Tjeng L H, van Elp J, Eskes H, Westerink J, Sawatzky G A *et al* 1988 *Phys. Rev. B* **38** 11322
[26] Shen Z X, List R S, Dessau D S, Parmigiani F, Arko A J, Bartlett R *et al* 1990 *Phys. Rev. B* **42** 8081